PAPER

Check for updates

Identification of H₂S/NO-donating artemisinin derivatives as potential antileukemic agents†

Xuemei Chen,[a] Pei Huang, [b] Jing Wang, [cd] Runmei Tian,[b] Yan Chen,*[b] Yongzheng Chen, [cd] Lei Zhang [*cd] and Zhigui Ma*[a]

Three H₂S/NO-donating artemisinin derivatives were designed and synthesized. Their antiproliferative activities were evaluated against human acute myeloid leukemia (AML) cell lines of K562 and K562/ADR and human normal liver cells of LO2. Biological evaluation indicated that NO-donating compound **10c** exhibited the most potent cytotoxicity against leukemia cells, similar to the bioactivity of clinical drug of homoharringtonine, but showed less toxicity than homoharringtonine against LO2 cells. Further mechanism studies revealed that **10c** could enhance the levels of intracellular NO and ROS, induce apoptosis and S phase cell cycle arrest, and disturb the mitochondrial membrane potential in K562 and K562/ADR cells. Western blot results demonstrated that **10c** noticeably promoted autophagy by up-regulating the levels of Beclin1 and L3-II expression, inhibited the AKT signaling, and stimulated the AMPK and JNK signaling in both leukemia cell lines. Overall, **10c** exhibited the potential to be a promising candidate for the therapy of AML.

Introduction

Leukemia, a cancer of the blood or bone marrow, is the ninth most common cancer in the United States.[1] Leukemia can be clinically classified into four major kinds: acute lymphoblastic leukemia (ALL), chronic lymphocytic leukemia (CLL), acute myeloid leukemia (AML), and chronic myeloid leukemia (CML). AML is the most common type of acute leukemia in adults. There are several possible treatments for AML, such as allogeneic bone marrow transplantation, which involves high-dose chemotherapy and radiation, as well as a high risk of death. Chemotherapy is another countermeasure for newly diagnosed patients with AML, such as cytotoxic drugs (adriamycin and homoharringtonine). However, the resistance to chemotherapy drugs has developed in a significant portion of AML patients.[2] Therefore, it is necessary to develop a novel strategy or drug for treatment of AML.[3]

[a]Department of Pediatric Hematology, West China Second University Hospital, Sichuan University, Chengdu 610041, PR China. E-mail: zhiguima@scu.edu.cn

[b]Department of Pediatrics, Affiliated Hospital of Zunyi Medical University, Zunyi 563003, PR China. E-mail: cyz600@163.com

[c]Key Laboratory of Biocatalysis & Chiral Drug Synthesis of Guizhou Province, School of Pharmacy, Zunyi Medical University, Zunyi 563003, PR China. E-mail: lzhang@zmu.edu.cn

[d]Key Laboratory of Basic Pharmacology of Ministry of Education, Joint International Research Laboratory of Ethnomedicine of Ministry of Education, Zunyi Medical University, Zunyi 563003, PR China

Artemisinin (**1**, Fig. 1), a naturally occurring sesquiterpene lactone isolated mainly from *Artemisia annua* L., had been used as a traditional Chinese medicine for treating malaria hundreds years ago.[4] Nowadays, numerous derivatives of artemisinin have been synthesized, and several artemisinin derivatives with less toxicity, improved solubility and enhanced antimalarial activity, such as dihydroartemisinin (**2**, Fig. 1) and artesunate (**3**, Fig. 1), have been used as first-line antimalarial drugs widely. Besides, artemisinin and its derivatives have been shown to exhibit significantly antineoplastic activities *in vitro* and *in vivo*.[5] Furthermore, they showed antiproliferative activities towards various human cancer cells, such as U937, NB-4, PC-3, MDA-MB-231 and MCF-7.[6] Particularly, dihydroartemisinin and artesunate were promising candidates for leukemia treatment due to its potential anticancer activity in leukemic cell lines and murine models.[7,8] Recently, our group also reported that artesunate and its derivative displayed anticancer activity against leukemia cells *in vitro* and *in vivo*.[9,10] In addition, some studies have shown that artemisinin and its derivatives could be used as sensitizers to improve the cytotoxicity of other chemotherapeutic drugs.[11,12] However, up to now, there were no artemisinin
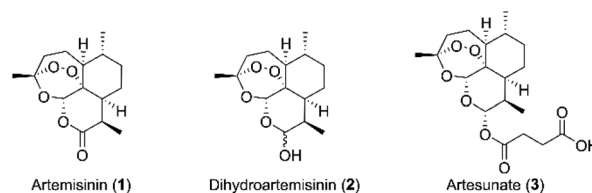

Fig. 1 The structures of artemisinin and its derivatives.

derivatives or artemisinin derivatives in combination chemotherapy had entered into clinical trials for the treatment of leukemia.

Hydrogen sulfide (H_2S), nitric oxide (NO) and carbon monoxide (CO), are increasingly recognized as important endogenous mediators of diverse physiological processes, such as vasodilation and neuromodulation.[13] H_2S was reported to regulate protein kinases such as p38 mitogen-activated protein kinase and trigger cell apoptosis at concentration of 20 μM.[14] There are several kinds of donor molecules which can release H_2S under physiological conditions, such as inorganic salts (NaHS and Na_2S). The drawback in using salts as H_2S donors is the uncontrolled release profile. Therefore, many small organic compounds have been designed and synthetized for releasing H_2S via endogenous enzymatic and/or non-enzymatic pathways, including 5-(4-hydroxyphenyl)-3H-1,2-dithiole-3-thione (ADT-OH, **4**, Fig. 2) and 4-hydroxy benzothiazamide (TBZ, **5**, Fig. 2).[15] Some reports had pointed out that H_2S donors also displayed antitumor effects.[16] Meanwhile, a number of synthetic H_2S releasing molecules have been shown to exhibit anticancer activities in vitro and in vivo.[17] Moreover, NO is a renowned gasotransmitter with a variety of physiological roles.[18] Previous studies have reported that high levels of NO could inhibit proliferation and survival of tumor cells, and sensitize tumors to chemotherapy in vitro and in vivo, by inhibition of key transcription factors, DNA repair enzymes and drug efflux pumps.[19,20] Like H_2S donors, NO donors also have gained great attention for decades owing to the high reactivity and inconvenient handling, which contain organic nitrates, diazeniumdiolates, S-nitrosothiols and furoxans.[21] For example, nitroglycerin (**6**), isosorbide 5-mononitrate (ISMN, **7**) and isosorbide dinitrate (ISDN, **8**) (Fig. 2) are organic nitrates, well-known vasodilators used in the therapy and prevention of angina pectoris by releasing NO,[22] as well as exhibit antitumor and enhance chemosensitivity.[23,24] Chen et al. demonstrated that the bioconversion of nitroglycerin to release NO occurred through mitochondrial enzyme aldehyde dehydrogenase 2 (ALDH2).[25] Moreover, JS-K (**9**, Fig. 2), an NO-donating diazeniumdiolate, released high levels of NO when suitably activated by glutathione or GST, and exhibited anticancer activity against various human cancer cell lines.[26,27] Particularly, Kodela and co-workers reported that NOSH-aspirin bearing both NO and H_2S-releasing moieties suppressed eleven different human cancer lines, and NOSH-1 was the most potent hybrid, with

an IC_{50} value of 48 nM in HT-29 cells.[28] In 2017, Gu et al. synthesized a series of NO-releasing bifendate derivatives, and further biological evaluation showed that the most potent compound significantly inhibited the proliferation of resistant K562/ADR cells in vitro and in vivo by releasing high levels of NO.[29]

Given that both H_2S/NO and artemisinin derivatives possess anticancer activity against various cancer cell lines, we hypothesized that the H_2S/NO-donating artemisinin derivatives could exert potent cytotoxicity. In this study, to find valid candidates for the treatment of AML, we designed and synthesized three H_2S/NO-donating artemisinin derivatives by coupling artesunate with H_2S donors (ADT-OH and TBZ) and NO donor (ISMN) using the molecular hybridization strategy (Fig. 3). We further evaluated these H_2S/NO-donating artemisinin derivatives for their antileukemic activities against AML cell lines, K562 and K562/ADR.

Results and discussion

The synthesis of hybrid molecules **10a–10c** is outlined in Scheme 1. Firstly, intermediate **3** was prepared according to the method described previously[30] via sodium borohydride ($NaBH_4$) catalyzed reduction reaction of artemisinin (**1**) and 4-dimethylaminopyridine (DMAP) catalyzed esterification reaction. Then, the target molecules were obtained in good yields by reacting **3** and different H_2S donors (**4** and **5**) or NO donor (**7**) via EDCI and DMAP catalyzed esterification reaction. The desired hybrid compounds were purified using column chromatography on silica gel and further characterized via ^1H NMR, ^{13}C NMR and high-resolution mass spectra (HRMS).

The antiproliferative activities of target hybrids (**10a–10c**) were performed against AML cell lines of K562 and K562/ADR and human normal hepatic LO2 cells by the CCK-8 assay in vitro initially, compared with lead compounds artemisinin (**1**), dihydroartemisinin (**2**), artesunate (**3**), H_2S releasing moieties (**4** and **5**), NO donor (**7**) and positive controls, homoharringtonine (**HHT**) and adriamycin (**ADR**). The IC_{50} values of test compounds were summarized in Table 1. All three H_2S/NO-donating artemisinin derivatives were notably effective in inhibiting the growth of two leukemic cell lines, which displayed more potent antiproliferative activities than three lead
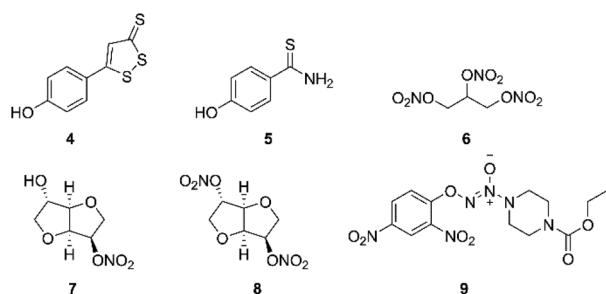

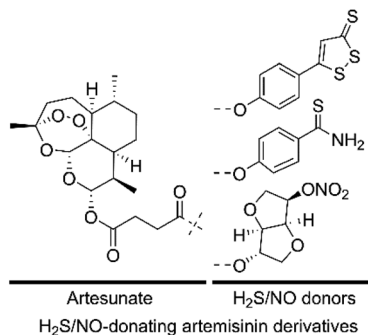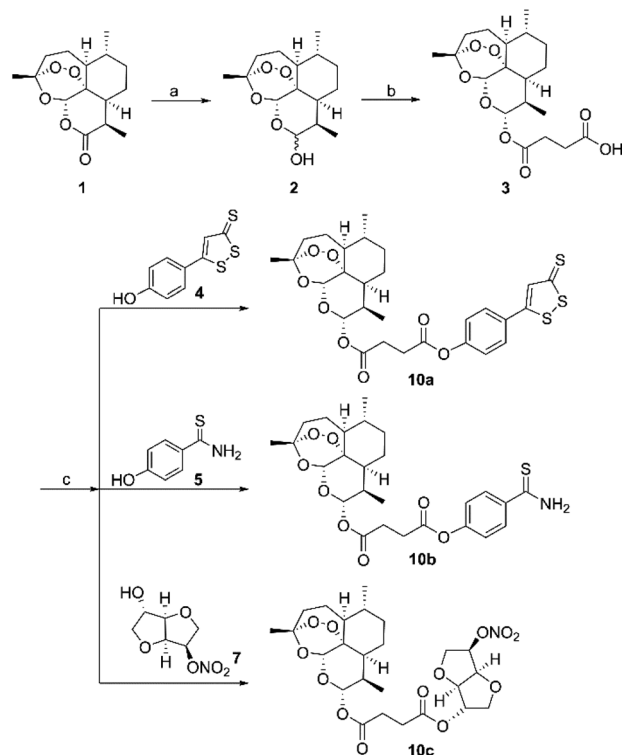**Fig. 2** The structures of H_2S/NO-donating agents.

Fig. 3 Design of H_2S/NO-donating artemisinin derivatives.

Scheme 1 Synthesis of H$_2$S/NO-donating artemisinin derivatives. Reagents and conditions: (a) NaBH$_4$, MeOH, 0–5 °C; (b) succinic anhydride, DMAP, DCM, rt; (c) EDCI, DMAP, DMF, rt.

compounds, artemisinin, dihydroartemisinin and artesunate. Nevertheless, all H$_2$S/NO donors showed weak inhibitory activity with IC$_{50}$ values more than 200 μM. Interestingly, hybrid **10c** incorporated with ISMN showed stronger activity than **10a** and **10b** with H$_2$S releasing moieties against both K562 and

Table 1 Antiproliferative activity of H$_2$S/NO-donating artemisinin derivatives *in vitro*

	IC$_{50}$^{a} (μM)		
Compd	K562	K562/ADR	LO2
1	11.085 ± 0.832	>200	83.341 ± 1.988
2	8.666 ± 0.277	28.068 ± 1.095	19.893 ± 1.66
3	10.17 ± 0.135	36.433 ± 2.902	19.864 ± 0.331
4	>200	>200	>200
5	>200	>200	>200
7	>200	>200	>200
10a	2.981 ± 0.391	16.632 ± 2.058	9.862 ± 0.479
10b	1.031 ± 0.116	8.479 ± 1.081	2.244 ± 0.359
10c	0.316 ± 0.021	6.634 ± 0.795	3.077 ± 0.281
HHT	0.367 ± 0.011	3.256 ± 0.082	0.915 ± 0.149
ADR	0.672 ± 0.056	9.161 ± 0.658	2.736 ± 0.123

^{a} The cells were treated with the indicated concentrations of each test compound for 72 h by the CCK-8 assay. The IC$_{50}$ value (drug concentration inhibiting 50% of the cell proliferation) for each compound was calculated and expressed as mean IC$_{50}$ (μM) ± SD from three independent experiments.

K562/ADR cells. In K562 cell line, **10c** showed similar inhibitory activity (IC$_{50}$ = 0.316 ± 0.021 μM) to clinical drug **HHT** (IC$_{50}$ = 0.367 ± 0.011 μM) and exhibited superior cytotoxic activity to positive control **ADR** (IC$_{50}$ = 0.672 ± 0.056 μM). Meanwhile, the inhibitory activity of hybrid **10c** (IC$_{50}$ = 6.634 ± 0.795 μM) against resistant K562/ADR cells was slightly stronger than that of **ADR** (IC$_{50}$ = 9.161 ± 0.658 μM), but slightly weaker than that of **HHT** (IC$_{50}$ = 3.256 ± 0.082 μM). Furthermore, in LO2 cells, NO releasing artemisinin derivative **10c** also showed lower cytotoxicity (IC$_{50}$ = 3.077 ± 0.281 μM) than two clinical drugs **HHR** (IC$_{50}$ = 0.915 ± 0.149 μM) and **ADR** (IC$_{50}$ = 2.736 ± 0.123 μM), suggesting that target compound **10c** may be a promising candidate for further investigation.

Compound **10c** was composed of artesunate moiety (**3**) and ISMN moiety (**7**) (Scheme 1), and the IC$_{50}$ values (shown in Table 1) of **10c** for K562 (IC$_{50}$ = 0.316 ± 0.021 μM) and K562/ADR cells (IC$_{50}$ = 6.634 ± 0.795 μM) were significantly less than that of individual moieties, **3** (IC$_{50}$ = 10.17 ± 0.135 and 36.433 ± 2.902 μM) and **7** (IC$_{50}$ > 200 and 200 μM), respectively. Furthermore, in order to investigate the antiproliferative activity of the combination of **3** and **7**, the growth inhibition of compounds **3**, **7**, and **3** + **7** against K562 and K562/ADR cells were determined by the CCK-8 assay. As seen in Fig. 4, it was notable that compounds **3** and **7** at 0.3 and 6 μM displayed less potent activity in both K562 and K562/ADR cell lines, respectively, however, conjugate **10c** exhibited 2.98-fold and 2.67-fold increase in its antiproliferative activity on K562 and K562/ADR cells comparable to the combination of **3** and **7**, respectively. These results suggested that the antitumor activity of hybrid **10c**
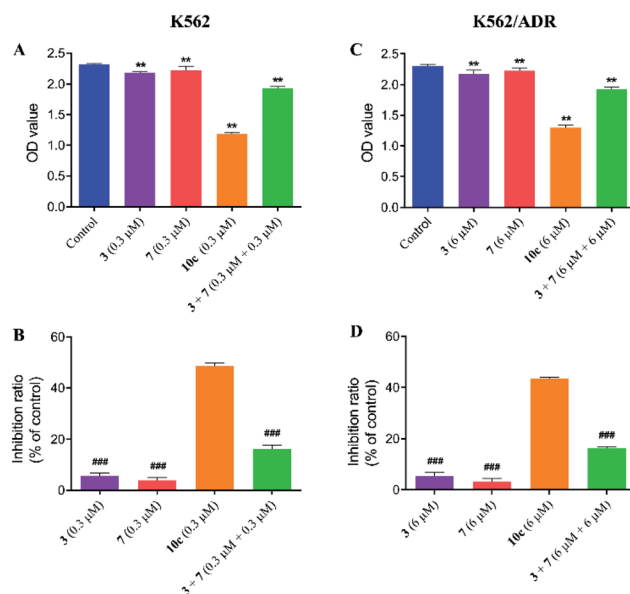

Fig. 4 Compounds **3**, **7**, **10c** and **3** + **7** inhibited the proliferation of K562 and K562/ADR cells. K562 cells were incubated with vehicle, **3** (0.3 μM), **7** (0.3 μM), **10c** (0.3 μM) and **3** + **7** (0.3 μM + 0.3 μM) for 72 h, and K562/ADR cells were incubated with vehicle, **3** (6 μM), **7** (6 μM), **10c** (6 μM) and **3** + **7** (6 μM + 6 μM) for 72 h, respectively. The cell proliferation was measured by CCK-8. Data were expressed as the means ± SD from three independent experiments. **P < 0.01 vs. the control group; ###P < 0.001 vs. the **10c** group.

may be attributed to the synergic effects of artesunate and NO donor moiety in cancer cells.

It was reported that high levels of NO could result in nitrosative stress (NS) and induce tumor cell apoptosis.[31] In order to verify the effect of NO on the anticancer activity of **10c**, the intracellular NO levels were first determined using DAF-FM DA as a cell permeable fluorescent probe. K562 and K562/ADR cells were incubated with vehicle, **10c** (1 μM, 10 μM and 100 μM), **3** (100 μM) and **7** (100 μM) for 3 h, respectively. And we measured NO generation by using fluorescence microscopy (Fig. 5A and C) and microplate reader (Fig. 5B and D), respectively. The results showed that hybrid **10c** promoted the generation of NO in both K562 and K562/ADR cells in a dose-dependent manner compared with the control group. Notably, the parents **3** and **7** also increased the intracellular NO levels, however, the effects of **3** and **7** were significantly weaker than that of **10c** in both K562 and K562/ADR cells, respectively, suggesting that the levels of intracellular NO induced by different compounds might be positively correlated with their antiproliferative activities. Furthermore, it was observed that treatment with test compounds caused lower levels of NO production in resistant K562/ADR cells, which might be associated with their anticancer activities in sensitive and resistant cancer cell lines. Interesting, parent **3** without NO donor also enhanced the intracellular NO levels, which may be related to previous study that the production of NO could be induced by inducible nitric oxide synthase (iNOS).[32]

Reactive oxygen species (ROS) are cellular metabolites and play vital roles in cellular homeostasis. In addition, more evidences suggested that the excessive generation of ROS contributed to apoptosis and autophagy in various tumor cells.[33] Extensive studies have showed that artemisinin and its derivatives induced apoptosis by ROS generation mediated by endoperoxide bridges.[5] Therefore, in this study, the generation of intracellular ROS in K562 and K562/ADR cells was investigated by fluorescence microscopy and flow cytometer after DCFH-DA staining, respectively. Cells were incubated with vehicle, **10c** (1 μM, 5 μM and 10 μM) and **3** (10 μM) for 24 h, respectively. As shown in Fig. 6A and D, **10c**-treated groups gave rise to increase in green fluorescence intensity in a dose-dependent manner, suggesting that **10c** heightened the levels of intracellular ROS. Simultaneously, as the increased concentrations of **10c**, the ROS production and percentage of ROS were gradually increased in K562 and K562/ADR cells (Fig. 6B, C, E and F). Moreover, incubation with **10c** caused higher levels of ROS production in sensitive K562 cells compared with that in resistant K562/ADR cells. Nevertheless, NO and ROS were reported to react to form peroxynitrite (ONOO−).[34,35] So, the correlation between NO and ROS induced by **10c** needs our further studies.

Cell cycle progression is vital to the cell processes, such as cell division and replication. Cell cycle arrest could inhibit cancer cell proliferation. Accumulating reports had reported that artemisinin derivatives inhibited cancer cells *via* cell cycle arrest.[36] To examine the antineoplastic mechanism of **10c** on
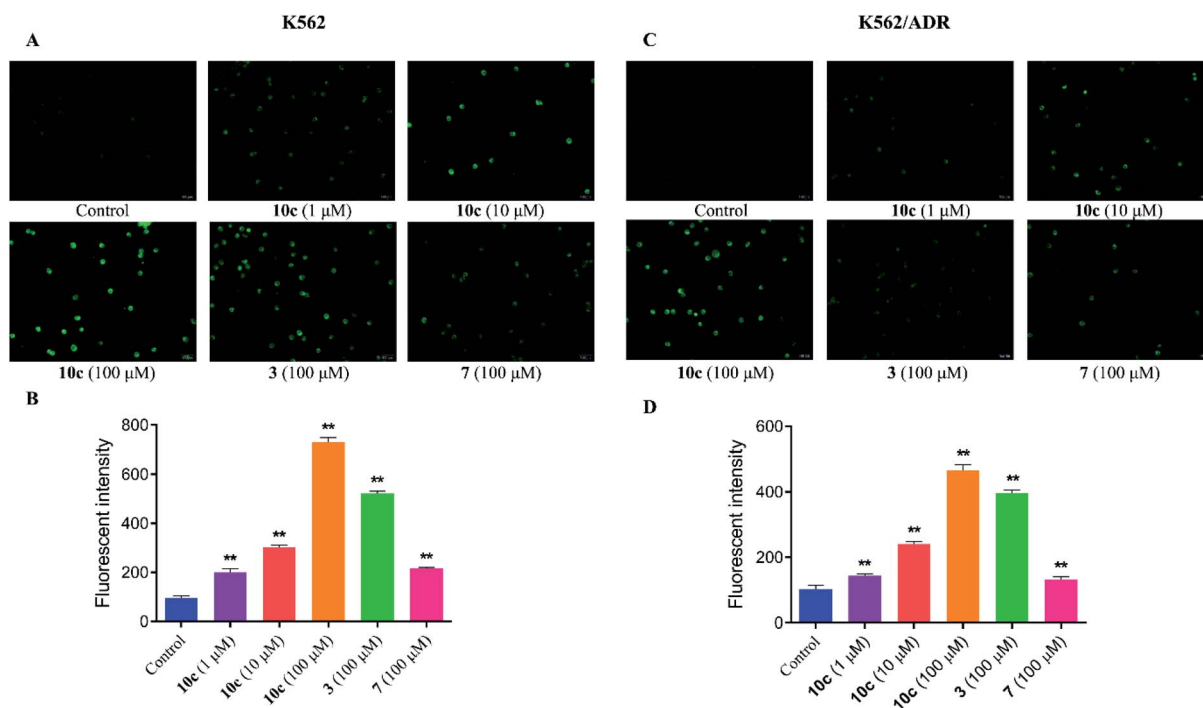

Fig. 5 The generation of intracellular NO in K562 and K562/ADR cells. Cells were incubated with vehicle, **10c** (1 μM, 10 μM and 100 μM), **3** (100 μM) and **7** (100 μM) for 3 h, respectively. (A and C) Intracellular NO was measured using DAF–FM DA staining by fluorescence microscopy. (B and D) NO production was assessed by microplate reader. The data were expressed as the mean ± SD from three independent experiments. **$*P < 0.01$ *vs.* the control group.
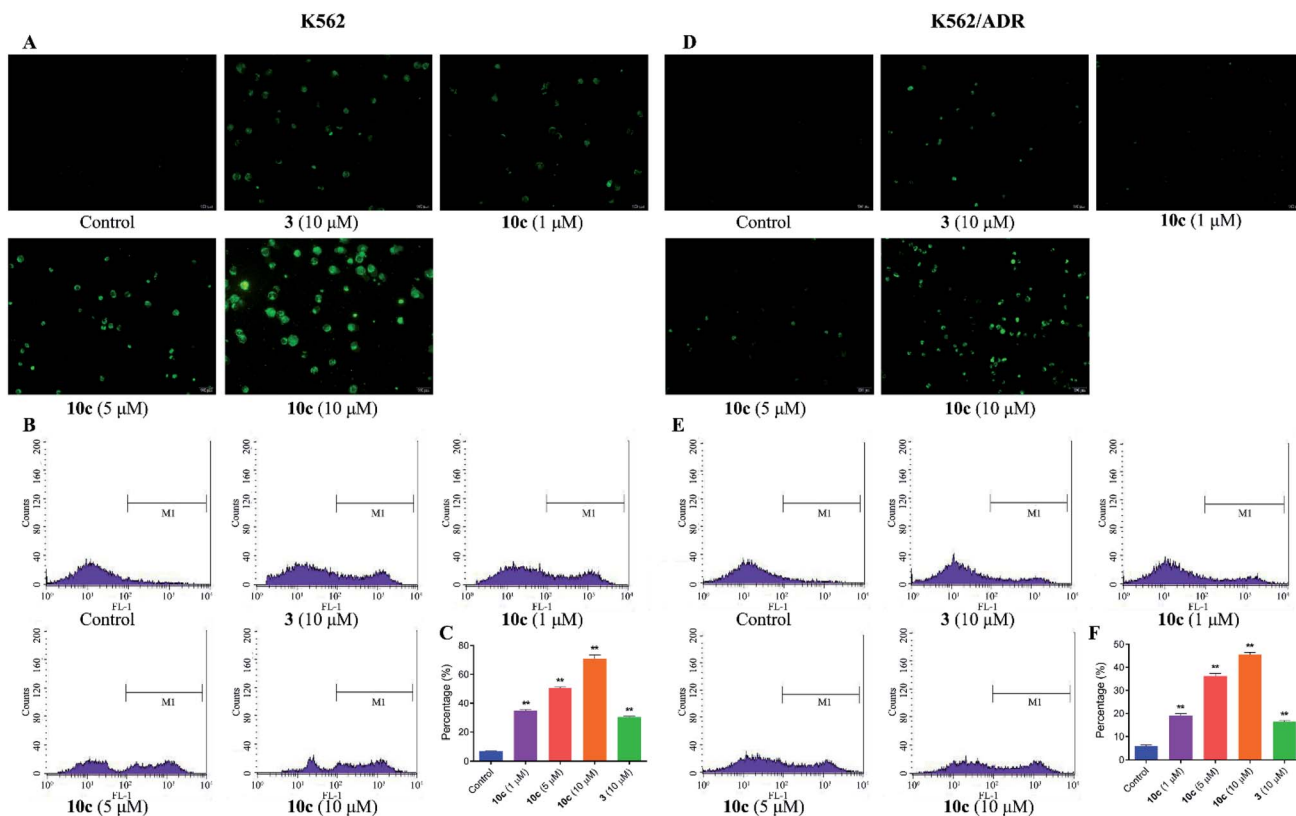
Fig. 6 The generation of intracellular ROS in K562 and K562/ADR cells. Cells were incubated with vehicle, **10c** (1 μM, 5 μM and 10 μM) and **3** (10 μM) for 24 h, respectively. (A and D) Intracellular ROS was measured using DCFH–DA staining by fluorescence microscopy. (B, C, E and F) ROS production and percentage of ROS were measured by flow cytometer, respectively. The data were expressed as the mean ± SD from three independent experiments. **$P < 0.01$ vs. the control group.

cell cycle, cell cycle distribution was measured using flow cytometry after staining with PI. K562 and K562/ADR cells were incubated with vehicle, **10c** (1 μM, 5 μM and 10 μM) and **3** (10 μM) for 24 h, respectively. As shown in Fig. 7, treatment of K562 and K562/ADR cells with **10c** resulted in accumulation at the S phase a concentration-dependent manner, respectively, compared with the control group. Meanwhile, the levels of the accumulation of K562 cells in the S phase after treatment with **10c** were slightly higher than the levels of the accumulation of K562/ADR cells.

Previous studies have shown that artemisinins and its derivatives can induce cancer cell apoptosis by modulating the expression of apoptosis-related regulators and signal events. Accordingly, to further confirm the effect of **10c** on induction of cancer cell apoptosis, K562 and K562/ADR cells were incubated with vehicle, **10c** (1 μM, 5 μM and 10 μM) and **3** (10 μM) for 24 h, respectively, and the percentages of apoptotic cells were measured by flow cytometry after staining with Annexin V-FITC and 7-AAD. As shown in Fig. 8, treatment with **10c** induced apoptosis in both K562 and K562/ADR cells in a dose-dependent manner, and **10c** at 10 μM showed significantly stronger effect than that of **3** in both K562 and K562/ADR cell lines.

It was reported that the loss of mitochondrial membrane potential (MMP) was a significant marker of mitochondrial dysfunction and played a key role in the process of cell

apoptosis.[37] To uncover the involvement of mitochondria pathway in **10c** induced apoptosis, the changes of mitochondrial membrane potentials were assessed in this paper. K562 and K562/ADR cells were incubated with vehicle, **10c** (1 μM, 5 μM and 10 μM) and **3** (10 μM) for 24 h, respectively, and further stained with fluorochrome JC-1 dye followed by flow cytometry analysis. Fig. 9 showed that **10c** obviously disturbed the mitochondrial membrane and decreased MMP in a dose-dependent manner in K562 and K562/ADR cells, which indicated that **10c** could induce cell apoptosis through mitochondria pathway. At the same time, mitochondrial membrane potential in K562 cells was more sensitive to **10c** than that in resistant K562/ADR cells.

In an effort to explore the molecular mechanisms underlying the **10c**-induced cell cycle arrest and apoptosis, we determined the regulatory effects of **10c** on the cycle- and apoptosis-related proteins in K562 and K562/ADR cells. Cells were incubated with vehicle, **10c** (1 μM, 5 μM and 10 μM) and **3** (10 μM) for 24 h, respectively, and the relative levels of CDK1, CDK2, cleaved caspase-3 and cleaved PARP expression were measured by western blot. After 24 h treatment with **10c**, suppression of CDK1 and CDK2 proteins expression, and up-regulation of cleaved caspase-3 and cleaved PARP proteins expression were observed in a concentration-dependent manner compared with the control group (Fig. 10), and the effects of **10c** were significantly stronger in K562 cells than those in K562/ADR cells.
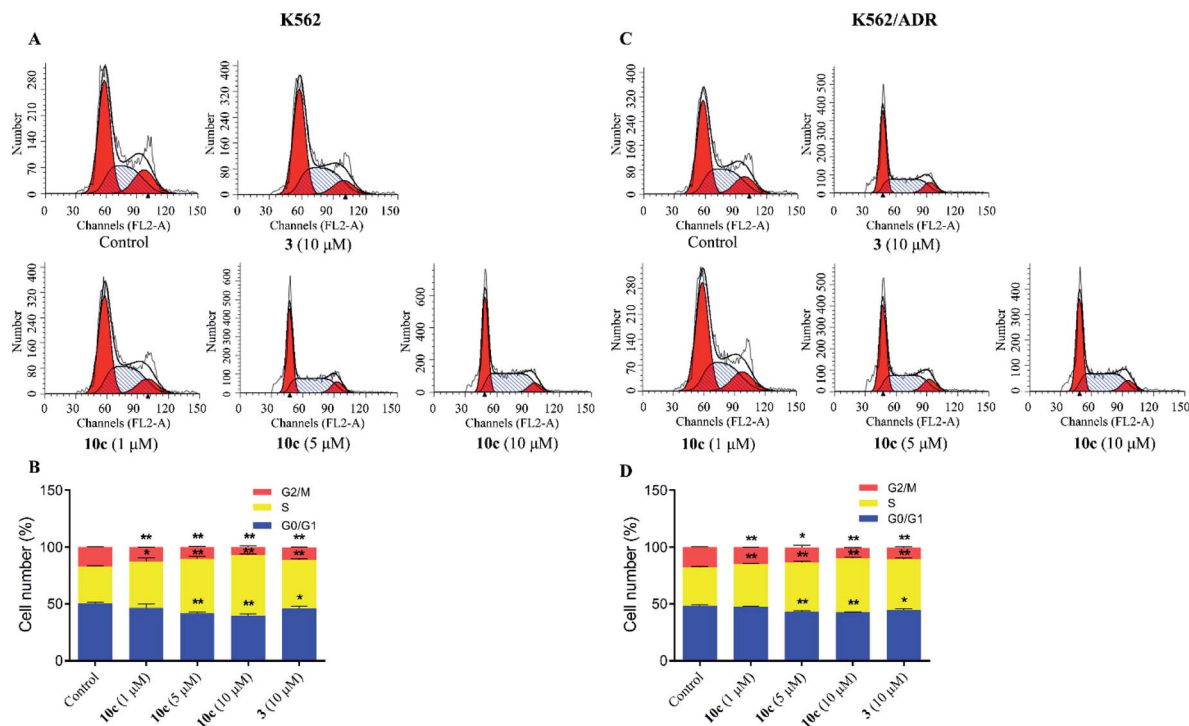
Fig. 7 Cell cycle arrest effects of compound **10c**. K562 and K562/ADR cells were incubated with vehicle, **10c** (1 µM, 5 µM and 10 µM) and **3** (10 µM) for 24 h, respectively, and cell cycle distribution was measured using flow cytometry after staining with PI. The data were expressed as the mean ± SD from three independent experiments. (A and C) Flow cytometry analysis. (B and D) Quantitative analysis. *$P < 0.05$, **$P < 0.01$ vs. the control group.
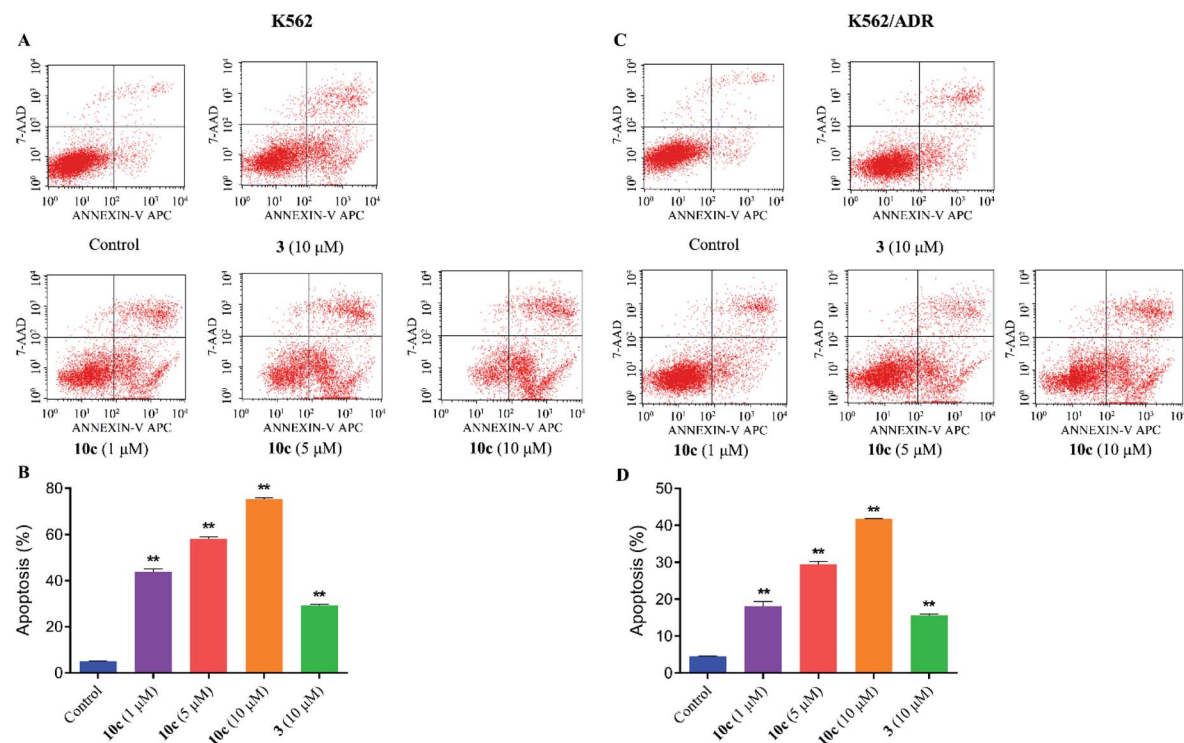

Fig. 8 Compound **10c** induced leukemia cells apoptosis. K562 and K562/ADR cells were incubated with vehicle, **10c** (1 µM, 5 µM and 10 µM) and **3** (10 µM) for 24 h, respectively, and the percentages of apoptotic cells were measured by flow cytometry after staining with Annexin V-FITC and 7-AAD. The data were expressed as the mean ± SD from three independent experiments. (A and C) Flow cytometry analysis. (B and D) Quantitative analysis. **$P < 0.01$ vs. the control group.

Fig. 9 Effects of **10c** on the mitochondrial membrane potential. K562 and K562/ADR cells were incubated with vehicle, **10c** (1 μM, 5 μM and 10 μM) and **3** (10 μM) for 24 h, respectively, and stained with JC-1 dye followed by flow cytometry analysis. The data were expressed as the mean ± SD from three independent experiments. (A and C) Flow cytometry analysis. (B and D) Quantitative analysis. **P < 0.01 vs. the control group.
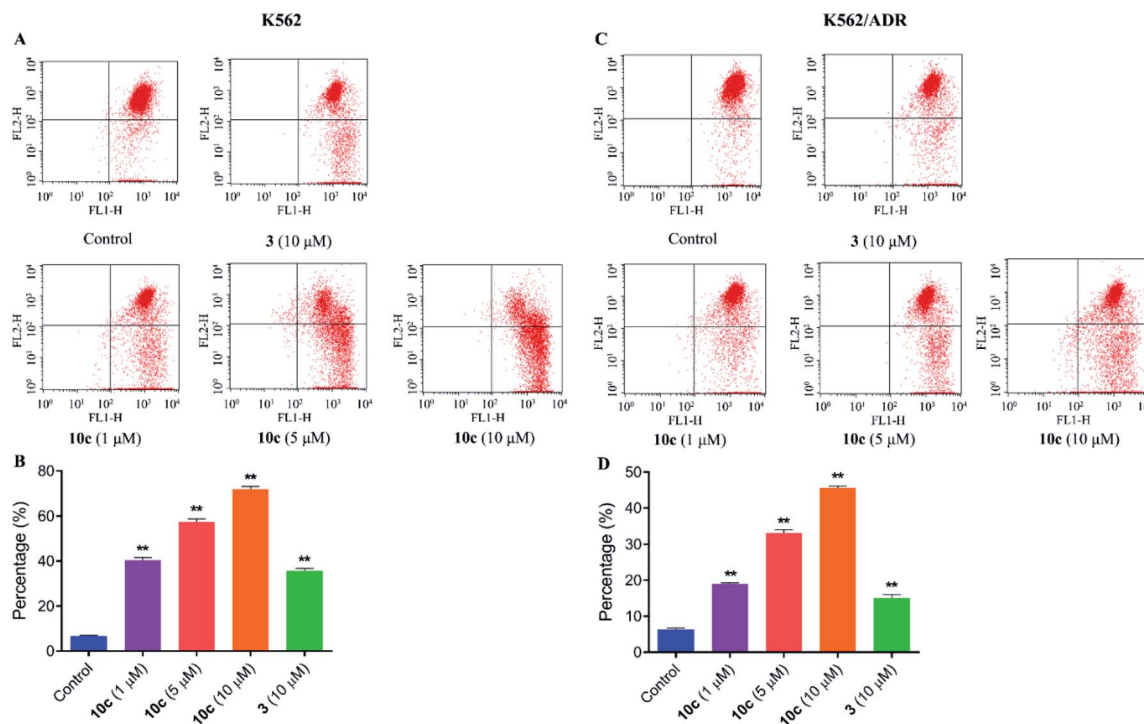
Besides apoptosis, autophagy is another programmed cell death, which plays a dual role in the cancer therapy.[38] Autophagy could induce cell death or protect cells depending upon the cell type and context.[39] Therefore, to assess whether autophagy contributes to **10c**-mediated inhibition of leukemia cell proliferation, we investigated the effects of **10c** on levels of the autophagy-related proteins in K562 and K562/ADR cells. Cells were incubated with vehicle, **10c** (1 μM, 5 μM and 10 μM) and **3** (10 μM) for 24 h, respectively, and the relative levels of Beclin1 and LC3-II expression were determined by western blot. After treatment with **10c**, the Beclin1 and cleavage of LC3 (LC3-II) levels were increased in a dose-dependent manner in K562 and K562/ADR cells (Fig. 11). We found that the level of autophagy in resistant K562/ADR cells was lower than that in sensitive K562 cells, and the **10c**-induction of autophagy were weaker in K562/ADR cells than those in K562 cells.

The crosstalk between apoptosis and autophagy is quite complex and remains controversial.[40] Apoptosis and autophagy may be activated by the common upstream signals, giving rise to the activation of the combination of autophagy and apoptosis,[41] such as AMPK, JNK and AKT signaling. Autophagy and apoptosis can be promoted by AMP activated protein kinase (AMPK), which is a key energy sensor and regulates cellular metabolism to maintain energy homeostasis,[42] and c-Jun N-terminal kinase (JNK), which is a stress-activated protein kinase (SAPK) of the mitogen activated protein kinase (MAPK) family.[43] Meanwhile, AKT is a serine/threonine protein kinase showing antiapoptotic activity, as well as inhibiting autophagy

mediated by activation of mTOR, which is a negative regulatory axis of autophagy.[44] To further explore the molecular mechanisms underlying the antiproliferative activity of **10c**, we investigated the regulatory effects of treatment with **10c** on the AMPK, JNK and AKT signaling in K562 and K562/ADR cells. Cells were incubated with vehicle, **10c** (1 μM, 5 μM and 10 μM) and **3** (10 μM) for 24 h, respectively, and the relative levels of AMPK, JNK and AKT phosphorylation were determined by western blot using β-actin as internal standard. As shown in Fig. 12, incubation with **10c** significantly inhibited the AKT phosphorylation and stimulated the AMPK and JNK phosphorylation in a dose-dependent manner in both cancer cell lines. Similarly, treatment with **3** also clearly reduced the levels of AKT phosphorylation and up-regulated the levels of AMPK and JNK phosphorylation, while the regulatory effects of parent **3** (10 μM) in both cell lines were noticeably less than that of **10c** (10 μM).

Experimental

General

Commercially available reagents and solvents were analytical grade and used without further purification. ^{1}H NMR and ^{13}C NMR spectra were recorded with an Agilent 400 NMR spectrometer, using TMS as an internal standard. High resolution mass spectrometry (HRMS) were obtained on an Agilent 6520 Accurate-Mass Q-TOF. Column chromatography was carried out on silica gel (200–300 mesh).
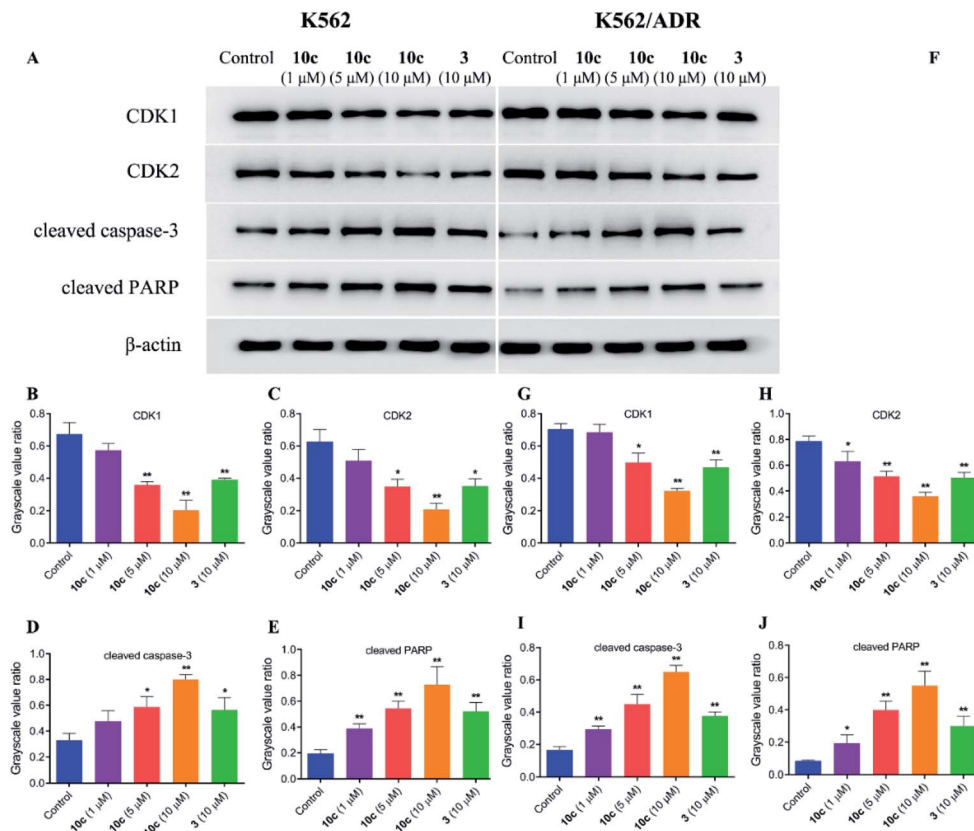
Fig. 10 Effects of **10c** on the cycle- and apoptosis-related proteins. K562 and K562/ADR cells were incubated with vehicle, **10c** (1 μM, 5 μM and 10 μM) and **3** (10 μM) for 24 h, respectively, and the relative levels of CDK1, CDK2, cleaved caspase-3 and cleaved PARP expression were determined by western blot using β-actin as internal standard. The data were selected images and expressed as the mean ± SD from three independent experiments. (A and F) western blot analysis, (B–E, G–J) quantitative analysis. *$P < 0.05$, **$P < 0.01$ vs. the control group.

General procedure for the preparation of hybrid compounds 10a–10c

Intermediate **3** (0.26 mmol) was dissolved in dry N,N-dimethylformamide (3 mL), then 1-(3-(dimethylamino)propyl)-3-ethylcarbodiimide hydrochloride (EDCI) (2.0 eq.), 4-dimethylaminopyridine (DMAP) (2.4 eq.), and appropriate donor (0.9 eq. for **4**, 0.95 eq. for **5** and **7**) were added. The reaction mixture was stirred at room temperature for 3–5 h. The reaction solution was quenched by adding water (20 mL), and the crude was filtered and dried in vacuum oven overnight. The crude residue was purified by silica gel flash column chromatography (dichloromethane/methanol 100 : 1 for **10a**, AcOEt/PE 1 : 4 for **10b** and 1 : 8 for **10c**) to afford the pure compound.

Hybrid compound **10a**: red solid, yield 63%; ^{1}H NMR (400 MHz, CDCl$_3$) δ 7.69 (d, $J = 8.4$ Hz, 2H), 7.40 (s, 1H), 7.28 (d, $J = 8.4$ Hz, 2H), 5.84 (d, $J = 10$ Hz, 1H), 5.46 (s, 1H), 2.99–2.84 (m, 4H), 2.61–2.56 (m, 1H), 2.43–2.35 (m, 1H), 2.06–2.02 (m, 1H), 1.93–1.88 (m, 1H), 1.80–1.64 (m, 4H), 1.43 (s, 3H), 1.40–1.30 (m, 3H), 1.25 (s, 1H), 0.98 (d, $J = 6.0$ Hz, 3H), 0.87 (d, $J = 6.8$ Hz, 3H); ^{13}C NMR (100 MHz, CDCl$_3$) δ 215.45, 171.77, 170.81, 170.26, 153.49, 135.98, 129.19, 128.21, 122.96, 104.50, 92.42, 91.51, 80.09, 51.48, 45.15, 37.25, 36.15, 34.01, 31.77, 29.67, 29.14, 29.12, 25.93, 24.54, 21.96, 20.19, 12.07; HRMS-ESI (m/z): calcd for C$_{28}$H$_{33}$O$_8$S$_3$ [M + H]$^+$ 593.1332, found 593.1335.

Hybrid compound **10b**: yellow solid, yield 78%; ^{1}H NMR (400 MHz, CDCl$_3$) δ 7.90 (d, $J = 8.8$ Hz, 2H), 7.75 (s, 1H), 7.38 (s, 1H), 7.15 (d, $J = 8.8$ Hz, 2H), 5.82 (d, $J = 10.0$ Hz, 1H), 5.46 (s, 1H), 2.95–2.81 (m, 4H), 2.60–2.54 (m, 1H), 2.42–2.34 (m, 1H), 2.06–2.02 (m, 1H), 1.90–1.87 (m, 1H), 1.80–1.70 (m, 3H), 1.65–1.60 (m, 1H), 1.54–1.46 (m, 1H), 1.42 (s, 3H), 1.39–1.26 (m, 3H), 0.97 (d, $J = 5.6$ Hz, 3H), 0.86 (d, $J = 7.2$ Hz, 3H); ^{13}C NMR (100 MHz, CDCl$_3$) δ201.37, 170.96, 170.43, 153.36, 136.68, 128.48, 121.52, 104.53, 92.44, 91.51, 80.12, 51.48, 45.14, 37.23, 36.15, 34.00, 31.76, 29.09, 25.90, 24.53, 21.95, 20.18, 12.05; HRMS-ESI (m/z): calcd for C$_{26}$H$_{34}$NO$_8$S [M + H]$^+$ 520.2000, found 520.2001.

Hybrid compound **10c**: white solid, yield 73%; ^{1}H NMR (400 MHz, CDCl$_3$) δ 5.80 (d, $J = 9.6$ Hz, 1H), 5.44 (s, 1H), 5.37–5.34 (m, 1H), 5.24 (d, $J = 2.8$ Hz, 1H), 5.00 (t, $J = 5.2$ Hz, 1H), 4.51 (d, $J = 5.2$ Hz, 1H), 4.06–3.97 (m, 3H), 3.93–3.89 (m, 1H), 2.73 (t, $J = 6.4$ Hz, 2H), 2.68–2.60 (m, 2H), 2.57–2.52 (m, 1H), 2.41–2.33 (m, 1H), 2.05–2.01 (m, 1H), 1.92–1.87 (m, 1H), 1.80–1.60 (m, 4H), 1.53–1.45 (m, 1H), 1.43 (m, 3H), 1.39–1.24 (m, 3H), 0.97 (d, $J = 6.0$ Hz, 3H), 0.86 (d, $J = 7.2$ Hz, 3H); ^{13}C NMR (100 MHz, CDCl$_3$) δ 171.08, 104.45, 92.27, 91.48, 86.43, 81.46, 81.30, 80.10, 77.60, 73.32, 69.22, 51.49, 45.17, 37.24, 36.16, 34.02, 31.79, 29.12, 28.88, 25.89, 24.53, 21.94, 20.19, 11.99; HRMS-ESI (m/z): calcd for C$_{25}$H$_{39}$N$_2$O$_{13}$ [M + NH$_4$]$^+$ 575.2447, found 575.2443.
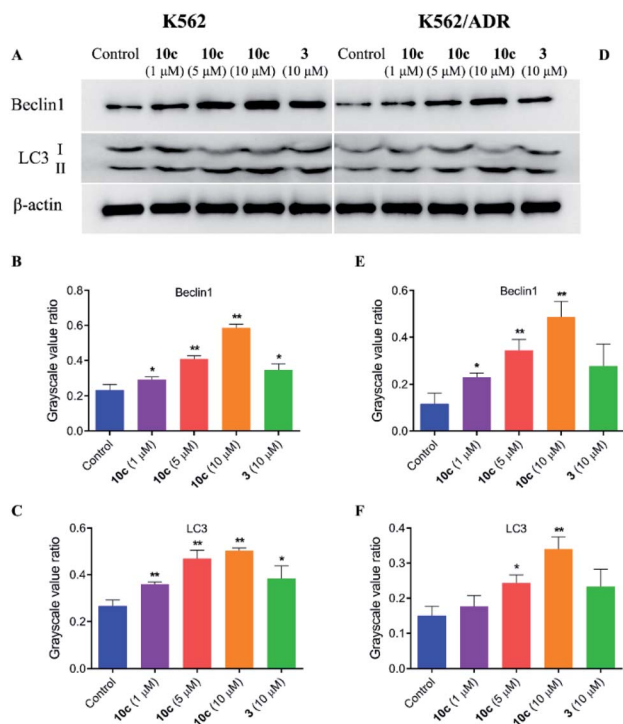
Fig. 11 Effects of **10c** on the autophagy-related proteins. K562 and K562/ADR cells were incubated with vehicle, **10c** (1 μM, 5 μM and 10 μM) and **3** (10 μM) for 24 h, respectively, and the relative levels of Beclin1 and LC3 expression were determined by western blot using β-actin as internal standard. The data were selected images and expressed as the mean ± SD from three independent experiments. (A and D) western blot analysis, (B, C, E and F) quantitative analysis. *P < 0.05, **P < 0.01 vs. the control group.

Fig. 12 Effects of **10c** on the AMPK, JNK and AKT signaling. K562 and K562/ADR cells were incubated with vehicle, **10c** (1 μM, 5 μM and 10 μM) and **3** (10 μM) for 24 h, respectively, and the relative levels of AMPK, JNK and AKT phosphorylation were determined by western blot using β-actin as internal standard. The data were selected images and expressed as the mean ± SD from three independent experiments. (A and E) western blot analysis, (B−D and F−H) quantitative analysis. *P < 0.05, **P < 0.01 vs. the control group.

Pharmacology

Cytotoxicity assay. The cytotoxicity of target compounds were tested against human acute myeloid leukemia K562 and K562/ADR cells and human normal hepatic LO2 cells *in vitro* by CCK-8 assay, respectively. The K562, K562/ADR and LO2 cell lines used in present study were purchased from KeyGen Biotech (Nanjing, China). Cells (2500–3000 cells per well) were cultured in 96-well plates and incubated at 37 °C for 24 h, and treated in triplicate with different concentrations of individual compounds for 72 h, and 0.1% DMSO for control. Then, CCK-8 (10 μL) was added to each well and plates were incubated at 37 °C for 2 h. The absorbance at 450 nm was measured using a microplate reader. The IC$_{50}$ value of each compound was calculated by GraphPad Prism version 6.01.

Measurement of intracellular NO. K562 and K562/ADR cells were incubated with 0.1% DMSO or different concentrations of test compounds at 37 °C for 3 h. Then cells were harvested and washed with PBS and then resuspended in incubation buffer containing fluorescein probe DAF-FM DA (50 μmol L^{-1}) at 37 °C for 30 min. The cells were washed with PBS and intracellular NO was analyzed by fluorescence microscopy and microplate reader, respectively. Each experiment was done three times.

Measurement of intracellular ROS. K562 and K562/ADR cells were incubated with 0.1% DMSO or different concentrations of
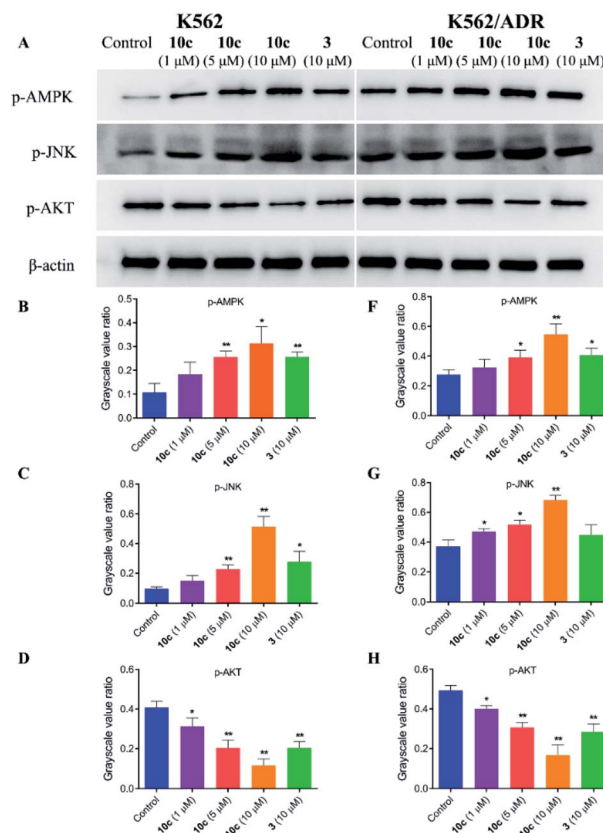
test compounds 37 °C for 24 h. Subsequently, cells were collected and washed with PBS, and then resuspended in incubation buffer containing fluorescein probe DCFH-DA (10 μmol L^{-1}) at 37 °C for 20 min. The cells were washed with PBS and intracellular NO was analyzed by fluorescence microscopy and flow cytometer, respectively. Each experiment was done three times.

Cell cycle analysis. K562 and K562/ADR cells were planted on 6-well plates and incubated overnight. Then cells were treated with 0.1% DMSO or different concentrations of test compounds 37 °C for 24 h. Cells were collected, washed twice with PBS, fixed with 70% ethanol at 4 °C for 2 h. Subsequently, cells were incubated with RNase A (100 μL) at 37 °C for 30 min, and then stained with propidium iodide (400 μL) at 4 °C in the dark for 30 min. The cell cycles were detected by flow cytometry. Each experiment was done three times.

Apoptosis analysis. K562 and K562/ADR cells were planted on 6-well plates and incubated overnight. Next, cells were treated with 0.1% DMSO or different concentrations of test compounds at 37 °C for 24 h. Cells were collected, washed twice with PBS and resuspended in binding buffer (500 μL).

Subsequently, cells were stained with Annexin V-FITC (5 μL) and 7-AAD (5 μL) at room temperature in the dark for 15 min. Cell apoptosis was analyzed by flow cytometer. Each experiment was done three times.

Mitochondrial membrane potential (MMP) analysis. K562 and K562/ADR cells were planted on 6-well plates and incubated overnight. Next, cells were treated with 0.1% DMSO or different concentrations of test compounds at 37 °C for 24 h. Cells were collected, washed with PBS and resuspended in incubation buffer containing JC-1 at 37 °C for 20 min. The stained cells were washed and analyzed by flow cytometer. Each experiment was done three times.

Western blot analysis. After treatment with 0.1% DMSO or different concentrations of test compounds for 24 h, cells were collected, washed with PBS and then lysed with lysis buffer. The total proteins were collected by centrifugation and determined by a Bradford assay. The protein was separated on 10–12% SDS-PAGE and transferred onto nitrocellulose membranes. The membranes were blocked with blocking buffer (TBST plus 5% skimmed milk) at room temperature for 2 h and then incubated with primary antibodies (CDK1, CDK2, cleaved caspase-3, cleaved PARP, Beclin1, LC3, p-AMPK, p-JNK, p-AKT or β-actin) at 4 °C overnight. After washing three times with TBST buffer, the cells then incubated with secondary antibody at room temperature for 2 h. Each band was visualized using enhanced chemiluminescence kit. Each experiment was done three times.

Statistical analysis. All experiments were conducted at least three times independently. The data were expressed as mean ± standard deviation. Statistical significance was analyzed by Student's t-test. $P < 0.05$ was considered statistically significant.

Conclusions

In summary, three H₂S/NO-donating artemisinin derivatives were synthesized and evaluated. Among them, NO-donating artemisinin derivative **10c** had potent inhibitory activity against AML cell lines of K562 and K562/ADR. In addition, compound **10c** was observed to increase the levels of intracellular NO and ROS, induce apoptosis and S phase arrest, and lessen the mitochondrial membrane potential in a concentration-dependent manner in K562 and K562/ADR cells. Moreover, **10c** could induce autophagy, activate AMPK and JNK signaling, and suppressed AKT signaling in both leukemia cell lines. We are also interested in further investigating the chemical mechanism of how NO improving activity of the parent. Overall, the data showed that **10c** may be a potential antileukemic candidate for the therapy of AML. Subsequently, we will further evaluate its stability *in vitro* and efficiency *in vivo*.

Conflicts of interest

There are no conflicts to declare.

Acknowledgements

Notes and references

1 R. L. Siegel, K. D. Miller and A. Jemal, *Ca-Cancer J. Clin.*, 2018, **68**, 7–30.

2 T. Arnason and T. Harkness, *Cancers*, 2015, **7**, 2063–2082.

3 V. M. Rumjanek, R. S. Vidal and R. C. Maia, *Biosci. Rep.*, 2013, **33**, 875–888.

4 L. H. Miller and X. Su, *Cell*, 2011, **146**, 855–858.

5 Y. K. Wong, C. Xu, K. A. Kalesh, Y. He, Q. Lin, W. S. F. Wong, H. M. Shen and J. Wang, *Med. Res. Rev.*, 2017, **37**, 1492–1517.

6 S. Luan, H. Zhong, X. Zhao, J. Yang, Y. Jing, D. Liu and L. Zhao, *Eur. J. Med. Chem.*, 2017, **141**, 584–595.

7 B. Kumar, A. Kalvala, S. Chu, S. Rosen, S. J. Forman, G. Marcucci, C. C. Chen and V. Pullarkat, *Leuk. Res.*, 2017, **59**, 124–135.

8 J. Lee, P. Shen, G. Zhang, X. Wu and X. Zhang, *Biomed. Pharmacother.*, 2013, **67**, 157–163.

9 L. Zhang, F. Chen, Z. Zhang, Y. Chen and J. Wang, *Bioorg. Med. Chem. Lett.*, 2016, **26**, 38–42.

10 M. Tan, Y. Rong, Q. Su and Y. Chen, *Leuk. Res.*, 2017, **62**, 98–103.

11 S. J. Wang, Y. Gao, H. Chen, R. Kong, H. C. Jiang, S. H. Pan, D. B. Xue, X. W. Bai and B. Sun, *Cancer Lett.*, 2010, **293**, 99–108.

12 L. Chen, C. Wang, N. Hu and H. Zhao, *RSC Adv.*, 2019, **9**, 1004–1014.

13 L. Li, A. Hsu and P. K. Moore, *Pharmacol. Ther.*, 2009, **123**, 386–400.

14 G. Yang, X. Sun and R. Wang, *FASEB J.*, 2004, **18**, 1782–1784.

15 E. G. Mueller, *Nat. Chem. Biol.*, 2006, **2**, 185–194.

16 R. Wang, *Physiol. Rev.*, 2012, **92**, 791–896.

17 Z. J. Song, M. Y. Ng, Z. W. Lee, W. Dai, T. Hagen, P. K. Moore, D. Huang, L. W. Deng and C. H. Tan, *RSC Med. Chem.*, 2014, **5**, 557–570.

18 L. J. Ignarro, *J. Physiol. Pharmacol.*, 2002, **53**, 503–514.

19 A. J. Burke, F. J. Sullivan, F. J. Giles and S. A. Glynn, *Carcinogenesis*, 2013, **34**, 503–512.

20 C. Riganti, E. Miraglia, D. Viarisio, C. Costamagna, G. Pescarmona, D. Ghigo and A. Bosia, *Cancer Res.*, 2005, **65**, 516–525.

21 A. W. Carpenter and M. H. Schoenfisch, *Chem. Soc. Rev.*, 2012, **41**, 3742–3752.

22 T. Münzel and T. Gori, *Curr. Opin. Pharmacol.*, 2013, **13**, 251–259.

23 E. Pipili-Synetos, A. Papageorgiou, E. Sakkoula, G. Sotiropoulou, T. Fotsis, G. Karakiulakis and M. E. Maragoudakis, *Br. J. Pharmacol.*, 1995, **116**, 1829–1834.

24 H. Yasuda, K. Nakayama, M. Watanabe, S. Suzuki, H. Fuji, S. Okinaga, A. Kanda, K. Zayasu, T. Sasaki, M. Asada, T. Suzuki, M. Yoshida, S. Yamanda, D. Inoue, T. Kaneta, T. Kondo, Y. Takai, H. Sasaki, K. Yanagihara and M. Yamaya, *Clin. Cancer Res.*, 2006, **12**, 6748–6757.

25 Z. Chen, J. Zhang and J. S. Stamler, *Proc. Natl. Acad. Sci. U. S. A.*, 2002, **99**, 8306–8311.

26 Z. Huang, L. Liu, J. Chen, M. Cao and J. Wang, *Biomed. Pharmacother.*, 2018, **107**, 1385–1392.

27 M. Z. Kaczmarek, R. J. Holland, S. A. Lavanier, J. A. Troxler, V. I. Fesenkova, C. A. Hanson, J. L. Cmarik, J. E. Saavedra, L. K. Keefer and S. K. Ruscetti, *Leuk. Res.*, 2014, **38**, 377–382.

28 R. Kodela, M. Chattopadhyay and K. Kashfi, *ACS Med. Chem. Lett.*, 2012, **3**, 257–262.

29 X. Gu, Z. Huang, Z. Ren, X. Tang, R. Xue, X. Luo, S. Peng, H. Peng, B. Lu, J. Tian and Y. Zhang, *J. Med. Chem.*, 2017, **60**, 928–940.

30 B. Xie, L. L. Meng, Y. J. Xiao, H. Y. Yang, B. L. Deng, S. Xiang and Y. Q. Kuang, *Chin. J. Synth. Chem.*, 2011, **19**, 62–65.

31 G. C. Brown and V. Borutaite, *Biochem. Soc. Trans.*, 2006, **34**, 953–956.

32 H. A. Lee, B. R. Song, H. R. Kim, J. E. Kim, W. B. Yun, J. J. Park, M. L. Lee, J. Y. Choi, H. S. Lee and D. Y. Hwang, *Exp. Ther. Med.*, 2017, **14**, 4986–4994.

33 J. Xu, Y. Wu, G. Lu, S. Xie, Z. Ma, Z. Chen, H. M. Shen and D. Xia, *Redox Biol.*, 2017, **12**, 198–207.

34 W. A. Pryor and G. L. Squadrito, *Am. J. Physiol.*, 1995, **268**, L699–L722.

35 Z. Xie, M. Wei, T. E. Morgan, P. Fabrizio, D. Han, C. E. Finch and V. D. Longo, *J. Neurosci.*, 2002, **22**, 3484–3492.

36 C. Morrissey, B. Gallis, J. W. Solazzi, B. J. Kim, R. Gulati, F. Vakar-Lopez, D. R. Goodlett, R. L. Vessella and T. Sasaki, *Anti-Cancer Drugs*, 2010, **21**, 423–432.

37 E. Gottlieb, S. M. Armour, M. H. Harris and C. B. Thompson, *Cell Death Differ.*, 2003, **10**, 709–717.

38 A. L. Edinger and C. B. Thompson, *Curr. Opin. Cell Biol.*, 2004, **16**, 663–669.

39 F. Nazio, F. Strappazzon, M. Antonioli, P. Bielli, V. Cianfanelli, M. Bordi, C. Gretzmeier, J. Dengjel, M. Piacentini, G. Fimia and F. Cecconi, *Nat. Cell Biol.*, 2013, **15**, 406–416.

40 G. Mariño, M. Niso-Santano, E. H. Baehrecke and G. Kroemer, *Nat. Rev. Mol. Cell Biol.*, 2014, **15**, 81–94.

41 J. M. Gump and A. Thorburn, *Trends Cell Biol.*, 2011, **21**, 387–392.

42 C. S. Zhang and S. C. Lin, *Cell Metab.*, 2016, **23**, 399–401.

43 X. Sui, N. Kong, L. Ye, W. Han, J. Zhou, Q. Zhang, C. He and H. Pan, *Cancer Lett.*, 2014, **344**, 174–179.

44 E. A. Dunlop and A. R. Tee, *Semin. Cell Dev. Biol.*, 2014, **36**, 121–129.